Relationship between spatial variations in static skin deformation and perceived roughness of macroscopic surfaces

Shogo Okamoto, *Member, IEEE,* Ariei Oishi

***Abstract*—The perceived roughness of macroscopic surface features is related to finger skin deformation. For example, skin indentation into surface grooves and the spatial variation in slowly adapting type 1 (SAI) mechanoreceptor activities are linked to the magnitude of subjective roughness. However, the perception of macroscopic roughness has not been directly linked to the spatial variations in skin deformation; therefore, this study investigated the relationship between the subjective roughness magnitude and the spatial spectrum of skin deformation through contact with roughened macroscopic surfaces. Experiments were performed to measure deformation of a finger pad when it statically touched different shaped grating scales. Then, the spatial spectra of skin deformation were computed by applying the Gabor filter with varying spatial selectivity. Some spectral components, particularly those for the spatial period ranging from 2.45–4.00 mm, exhibited a good correlation with the perceived roughness magnitude. When the optimal spatial periods were determined for individual subjects, the spectral components and perceived roughness exhibited a strong linear relationship with an average correlation coefficient of 0.94. Therefore, the amount of spatial variation in finger skin deformation can be linked to the subjective roughness intensities of macroscopic surface features.**

I. Introduction

The relationship between subjective roughness perception and surface features has been widely studied for surfaces with geometrically macroscopic features larger than approximately 1 mm. Previous research has successfully formulated surface feature functions, such as the groove width and spatial frequency of surfaces, to predict subjective roughness intensities (e.g. [1]–[7]). These studies agree that the groove width of gratings or the inter-element spacing of surface dots are the key factors that affect roughness perception, in that roughness intensities increase with the values of these factors. This phenomenon is attributed to skin deformation [8], i.e., the skin on a finger pad penetrates a wider groove to a larger depth. However, when groove width is larger than 3–4 mm, roughness intensities may not monotonically increase with groove width [5], [9]–[11] because the skin in the central part of a groove exhibits less deformation. Furthermore, if a groove is sufficiently shallow to enable an indented finger pad to reach the bottom (i.e., grove height is small), the skin does not penetrate the groove, which diminishes subjective roughness intensity [11].

According to neurophysiological studies, spatially macroscopic information is recorded by slowly adapting type 1 (SAI) units (e.g., [2], [12]–[15]), and spiking activities have previously been explained by the stress or strain of the skin tissue surrounding Merkel nerve endings [16]–[18]. The subjective roughness of specimens or material surfaces have been expressed by the spatial variation in SAI activities [3], [9], [19]–[21]. Spatial variation refers to the difference in activities between SAI units, in which receptive fields are closely located. Subjective roughness increases with the difference in activities.

Therefore, previous research has indicated that a relationship exists between the spatial variation or magnitude of skin deformation and roughness perception. For example, Taylor and Lederman [8] investigated how the cross-sectional area or depth of skin penetration into grooves can represent roughness perception. However, there is a lack of research that directly links the spatial variation in skin deformation and the perceived roughness of macroscopic surfaces.

Therefore, this study is designed to bridge the gap in the existing psychophysical and neurophysiological studies from the viewpoint of skin deformation. To achieve this goal, we performed experiments where human subjects pressed their finger pads on gratings with different shapes and widths larger than 1 mm. They appraised the grating scales without sliding motion following the framework of the magnitude estimation method. Then, spatial filters with specific frequency selectivities were applied to observed skin deformation images to compute spatial spectra, which were used to derive the spatial variation in skin deformation. The same filtering operation was performed on the spatial event plots of SAI units in earlier neurophysiological studies [3], [9], [19], [21], and spatial spectra were compared with subjective roughness intensities. The aim of this study is to determine how effectively skin deformation can statistically explain the subjective response to macroscopic surface roughness using a few types of grating scales.

We focus on static skin deformation because finger movement exhibits a relatively small effect on the judgment of macroscopic surface features [22]. In contrast, in terms of fine textures, the temporal aspects of skin deformation, i.e., skin vibration and subjective roughness, are closely linked (e.g., [21]–[23]).

A potential application of the outcome of this study is a roughness index based on skin deformation, even though the establishment of such an index is not the major objective of the present study. For numerous material developers and surface designers, it is expensive to repeat sensory appraisal and impractical to measure neural activity to evaluate roughness[1]. In contrast, it is simple to observe skin deformation. Therefore, this study provides an accessible method for evaluating roughness perception for macroscopic surfaces.

II. Methods

A. Stimuli

As shown in Fig. 1, 3D-printed (Form2, Formlabs, MA, stereolithography, minimal layer pitch: 25 μm) rectangular, triangular, and circular gratings were used as roughness samples. Rectangular and triangular gratings were frequently used in earlier studies (e.g., [2], [3], [5], [7]), whereas circular gratings were rarely used. We selected these three types of gratings to investigate if the spatial variation in skin is related to the subjective roughness of not only common grating scales but also other types of grating scales. We used *Tough v5* resin as a material. The rectangular gratings were defined by ridge and groove widths, whereas the triangular gratings were defined only by groove widths. The vertex angles of the triangles were 30°, 45°, or 60°. The circular gratings were defined by circular diameters and the interval of adjacent circles, where the latter was used only for gratings with small diameters. For all types of gratings, the depth of a groove

S. Okamoto and A. Oishi are with the Department of Mechanical Engineering Systems, Nagoya University, Japan. E-mail: okamoto-shogo@nagoya-u.jp

This study was in part supported by MEXT Kakenhi (#17H04697). The experimental protocols of this study were approved by the institutional review board of the School of Engineering, Nagoya University (#19-9).

[1]In future, fully or partially computerized simulations of unit activities are likely to be used widely [24], [25].

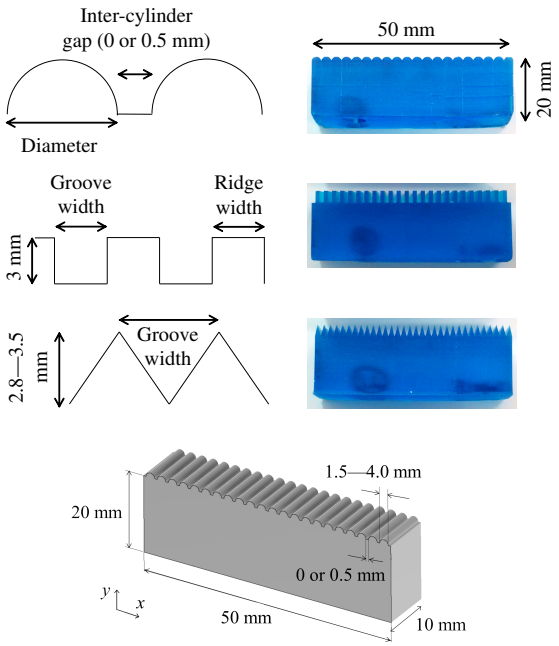

Fig. 1. Schematic diagrams and photographs of the gratings used as roughness samples. From top to bottom: circular, rectangular, and triangular gratings. The bottom three-dimensional drawing is a circular grating.

TABLE I
SPECIFICATIONS OF THE 16 GRATING TYPES USED IN THE EXPERIMENTS. VALUES IN PARENTHESES ARE USED FOR THE REGRESSION ANALYSIS.

Type	Ridge width (mm)	Groove width (mm)	Vertex angle	Circular diameter (mm)
Rectangular	0.75	1.0	-	-
	0.75	1.75	-	-
	1.0	1.0	-	-
	1.0	2.25	-	-
	1.5	1.5	-	-
Triangular	- (0)	1.5	30°	-
	- (0)	1.75	30°	-
	- (0)	2.5	45°	-
	- (0)	2.75	45°	-
	- (0)	3.5	60°	-
	- (0)	4.0	60°	-
Circular	- (0)	0.5 (1.5)	-	1.0
	- (0)	0.5 (1.75)	-	2.25
	- (0)	0 (2.5)	-	2.5
	- (0)	0 (3.0)	-	3.0
	- (0)	0 (4.0)	-	4.0

was designed to be sufficiently large such that the finger skin did not reach the bottom of the groove. Originally, 30 types of gratings were manufactured. From these, the gratings that allowed for the acquisition of clear images of skin deformation through the process described in Sec. II-E were selected. Gratings were also selected to ensure variable subjective roughness values. The specifications of the final 16 types of gratings are given in Table I. The dimensions of the roughness samples were $50 \times 20 \times 10$ mm.

B. Participants

Seven male university students in their 20s (age: 23 ± 1.5 years old) were recruited for this study. The students provided written informed consent. All subjects were right handed and declared no tactual disabilities. The subjects were unaware of the study objectives prior to the experiments.

C. Experiment: Subjective roughness magnitude

1) Procedure: The participants appraised the roughness magnitude of each sample according to a reference modulus stimulus. For example, if the roughness of a sample was perceived to be 1.5 times that of the modulus, then a value 1.5 times the modulus was assigned to the sample. The modulus was a triangular grating with a groove width of 1.0 mm (vertex angle of 30°), which was not included as an experimental grating. This grating was presented to the participants after consecutively presenting four test stimuli. For subjective inspection, each participant laid their thumb on a roughness sample, which was placed on an electric weight scale, and a load of ∼300 gf was maintained for a few seconds before reporting the intensity of the sample. Furthermore, the subjects were instructed not to slide their thumbs. These conditions were also employed to image skin deformation, as described in Sec. II-E. We used the thumb to photograph the large stable contact region. The roughness samples were presented to each subject in a randomized order, and each sample was tested three times per participant. The entire procedure required approximately 45 min for individuals, including the initial 5 min for practice.

2) Data analysis: For individuals, to prevent the effects of outliers on experimental results, the median values of the roughness magnitude were calculated from the three responses for each roughness sample. These median values were normalized such that their geometric mean was 1 among all types of gratings. We did not perform logarithmic transformation on these normalized values because, as discussed later, they exhibited a strong linear relationship with the groove width of the roughness samples and the spatial spectrum of skin deformation.

D. Regression analysis of perceived roughness via macroscopic surface features

The subjective roughness values were estimated using regression analysis by utilizing ridge width, groove width (GW), and the square of groove width as potential explanatory variables[2]. In terms of groove width, the values provided in parentheses in Table I were used, where the ridge widths for the circular and triangular gratings were zero. The net distance between circular peaks was used as the groove width of the circular gratings. For this analysis, the *stepwisefit* function of Matlab (Matlab2019a, MathWorks Inc., MA) was used with a statistical significance level of $p < 0.05$ for variable selection. The subjective roughness values averaged among the participants were utilized for this operation.

E. Image acquisition and processing

After magnitude estimation experiments, the participants again laid their right thumbs on each roughness sample, and a cross-sectional picture was obtained from the distal direction, i.e., from the tip, using a digital camera (RX-10II, Sony, Japan, 20.2 million pixels, macro-photography mode). Lighting conditions were adjusted so that the interface between the two materials was clear. Each participant maintained a finger load of 300 gf on the electric weight scale for the duration of image acquisition.

The images were processed using Gimp 2.10.12, as follows: Optically zoomed images were shrunk to achieve a unified resolution of 700 pixels per 10 mm, i.e., 0.014 mm/pix (Fig. 2a). The

[2] GW, GW^2, ridge width, and spatial wave length (GW + ridge width) are the potential predictors of subjective roughness [3], [5], [7], [26]. However, in our setup, for the triangular and most circular gratings, ridge width was zero and wave length and GW were equal. For such cases, either wave length or GW should be used to prevent the problem of collinearity, and we selected GW.

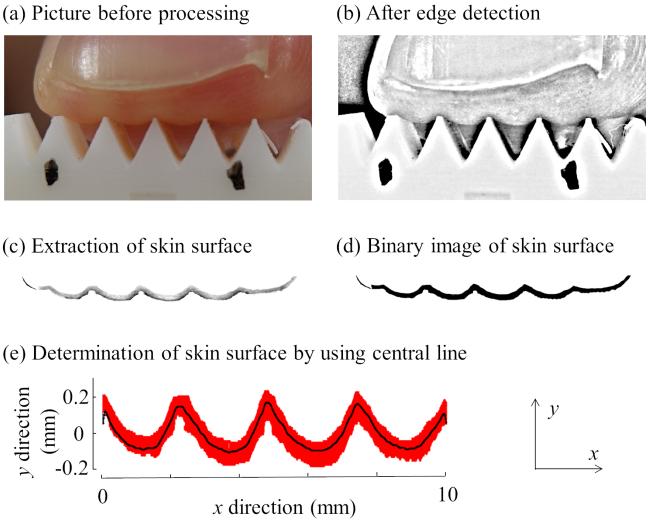

Fig. 2. Image processing procedure to determine the deformed skin surface line. (a) Cross-sectional image of thumb before image processing. (b) After applying edge detection to the image. (c) Selection of the skin surface using an automatic selector. (d) Black and white image of the skin surface region. (e) Central curve determined along the x-direction. Red dots represent the skin surface region acquired in (d). The image processing shown in (c)–(d) was conducted using Gimp 2.10.12.

brightness level was adjusted to clarify the boundary between the skin and grating, and the optical boundary was computed using the *photocopy* function (Fig. 2b). The skin boundary was extracted using the *intelligent scissors tool*, which automatically separates different objects in an image. The separated region was visually inspected and manually rectified if necessary (Fig. 2c). Then, the images were transformed into black and white binary images (e.g. Fig. 2d). The images were loaded into Matlab (Matlab 2019a, Mathworks, MA) to calculate the curve that passed through the center of the skin surface region in the x-direction, i.e., the red dots in Fig. 2e. Finally, quadratic and linear trends were removed from the curve and the skin boundary was acquired as a black curve (Fig. 2e). Skin boundary curves were acquired for each combination of participant and grating type, resulting in 112 curves.

F. Computation of the spatial spectra of static skin deformation

The one-dimensional Gabor filter was applied to the skin deformation curve. The two-dimensional version of this filter was used for the spatial event plots of SAI units in earlier studies [19]–[21]. Further, a similar operation was used in [3], [9].

The one-dimensional Gabor filter is a harmonic function with an attenuating amplitude, which functions as a filter with a peak sensitivity at the spatial period, λ mm, to compute the spectra of skin deformation. The profile of the filter is defined by

$$g(x) = \exp(\frac{-x^2}{2\sigma^2}) \cos(\frac{2\pi x}{\lambda}) \tag{1}$$

where σ determines the attenuation of the amplitude (Fig. 3a). This filter and the skin deformation curve, $y(x)$ (Fig. 3b), were convoluted along the x-axis:

$$s(x) = (g * y)(x). \tag{2}$$

As shown in Fig. 3c, the maximum absolute output value, $\max(|s(x)|)$, was used as a spectral component for λ in the latter computation.

Determining the optimal value of σ was outside the scope of this study. However, the range of values of σ tested in this study (σ = 0.9–1.4 mm), which was close to that used in [19], [21] (σ = 1.12 mm), did not substantially influence the computational results. Therefore, we adopted $\sigma = 1.1$ mm. In contrast, the optimal values of λ depended on individual subjects. The values of λ ranged from λ = 1.0–5.0 mm, which included the value (λ = 2.8 mm) used in [19], [21], where λ was determined to best explain subjectively reported roughness. In our study, within this range, the value of λ for each participant was determined to achieve the maximum correlation coefficient between subjective roughness values and spatial spectral components (also see the second paragraph in Sec. IV).

Fig. 4 shows a few examples of the computation with λ = 2.66 mm, which is the optimal value found in Sec. III-B. Larger skin deformation leads to larger filter outputs. Further, filter outputs increase as the spatial periods of the skin deformation become closer to λ.

III. Results

A. Relationship between surface features of roughness samples and subjective roughness

For the rectangular and triangular gratings, the *stepwisefit* function found that only groove width significantly affected subjective roughness ($t(7) = 15.95$, $p < 0.001$), and the regression equation was determined as follows:

$$R = 0.54GW \tag{3}$$

where R and GW are the subjective roughness value and groove width, respectively. The contributions of RW ($t(7) = -1.77$, $p = 0.11$) and GW^2 ($t(7) = -0.50$, $p = 0.63$) were not observed.

Whereas the above analysis was conducted by involving the geometric means of all the participants, we also computed the gradient of the regression line for each combination of the individual participants and types of grating scale. The gradients were statistically significant for 17 of the 21 cases (7 participants $\times$ 3 types of grating) with $p < 0.05$, and the other four cases had a $p < 0.10$, which means that the subjective roughness covaried with the groove width for most participants and types of grating scales.

Fig. 5a shows the relationship between the geometric mean of subjective roughness for all participants and the groove width of gratings. The subjective roughness of the rectangular and triangular gratings was closely correlated with GW, with a correlation coefficient of $r = 0.98$. This value was close to those obtained in previous studies where subjective roughness was estimated using the geometric parameters of macroscopic surface roughness, i.e., 0.99 in [3], 0.96 in [7], 0.99 in [5], and $>$ 0.99 in [26]. When regression analysis was conducted for individuals, the mean and standard deviation of their correlation coefficients was $r = 0.96 \pm 0.027$.

Including the circular, rectangular, and triangular gratings, the regression equation was

$$R = 0.41GW + 0.23 \tag{4}$$

with a correlation coefficient of $r = 0.87$. GW ($t(12) = 6.71$, $p < 0.001$) significantly affected subjective roughness, whereas RW ($t(12) = -1.59$, $p = 0.14$) and GW^2 ($t(12) = -0.67$, $p = 0.51$) did not. Fig. 5a shows that roughness intensities were overestimated for the circular gratings. This suggests that GW should only be used to estimate the subjective roughness of rectangular and triangular gratings but not circular gratings. It is noted that circular gratings were rarely used in previous studies.

Fig. 5b shows the individual variation in the relationships between groove width and subjective roughness for three participants and

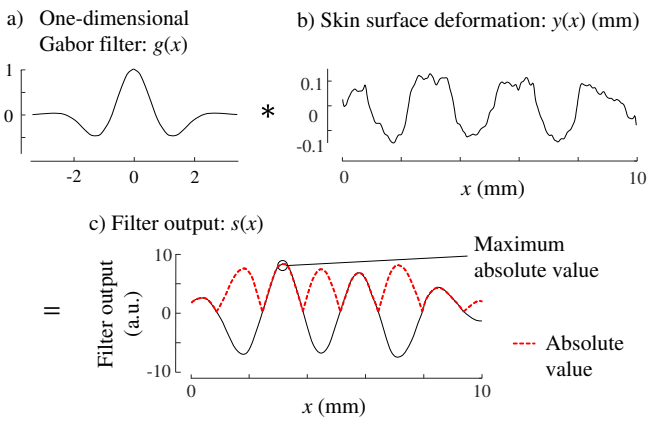

Fig. 3. Application of Gabor filter to the measured skin deformation. a) Gabor filter with spatial sensitivity designated by λ. b) Skin surface deformation. c) Output of the convolution on a) $g(x)$ and b) $y(x)$. The maximum absolute value was used as the spatial spectral component for λ.

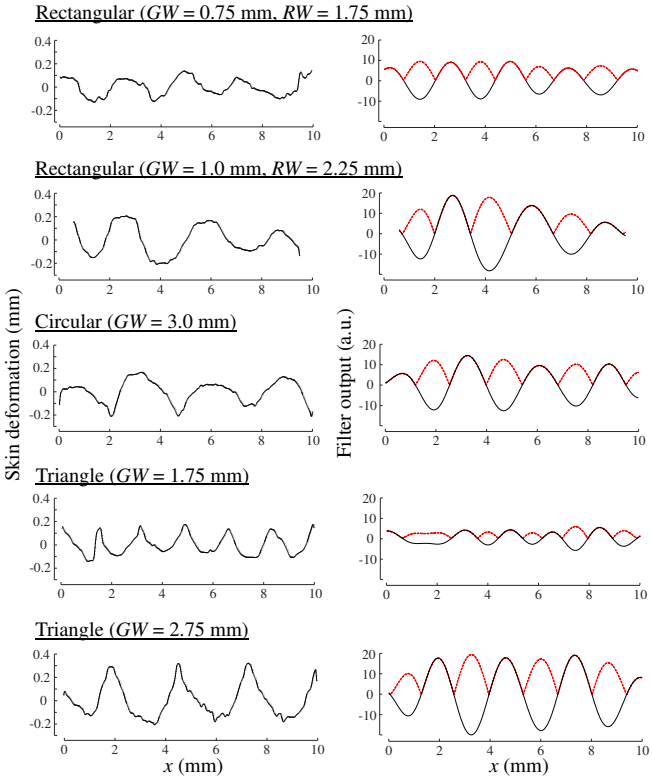

Fig. 4. Examples of skin deformation (left) and corresponding filter outputs (right) for four types of roughness samples. Red dotted curves are the absolute values. $\lambda = 2.66$ mm.

their regression lines. They include the highest and smallest gradients among those for all participants.

Even though the mean subjective roughness values for all participants were used in the above analyses, Fig. 5c shows the individual subjective intensities estimated by GW using all types of roughness samples, where the regression equation was established for each individual. The correlation coefficient ranged from 0.67–0.88 for all seven participants, with a mean and standard deviation of $r = 0.82 \pm 0.07$.

B. Relationship between subjective roughness and the spatial spectral component of skin deformation

Fig. 6a shows the relationships between spatial spectral components and subjective roughness for three example participants, where different colors correspond to different participants. A linear relationship was observed for all participants; however, the gradients of the linear fits and the distribution of roughness and spectral component values differed among the participants. These differences may indicate that spatial spectral components largely depend on the physical properties of individual finger pads, i.e., the softer the skin, the larger the skin deformation. The mean correlation coefficient between spectral components and subjective roughness among the seven participants was 0.85 ± 0.07, with maximum and minimum values of 0.93 and 0.72, respectively. This value was comparable to that between groove width and subjective roughness, i.e., 0.82 ± 0.07. Fig. 6b shows the mean values of subjective roughness and spatial spectral components for individual roughness samples. The means of these two values were closely correlated with a correlation coefficient of $r = 0.94$.

Roughness intensities were estimated using their linear relationships with the spatial spectral components of skin for each participant. Fig. 6c shows the relationship between estimated and reported roughness intensities. Even though the intensities of the circular gratings were overestimated when using groove width, as shown in Fig. 5a, the same trend was not observed when spatial spectral components were used. Instead, the roughness intensities of the triangular gratings tended to be underestimated, i.e., the majority were located above the 1:1 line.

As mentioned previously, the optimal values of λ for individual participants were used in the analysis. Fig. 7 shows the correlation coefficients between the spatial spectral components and subjective roughness for different values of λ for each individual (upper panel) and the means and standard deviations (lower panel). The value of λ that exhibited the peak correlation coefficient differed among the participants. The optimal values of λ ranged from 1.15–3.50 mm, and the mean was 2.66 mm.

IV. Discussion

Subjective roughness intensities were accurately estimated using the groove widths and spatial spectral components of skin deformation (Figs. 5 and 6, respectively). The results could suggest that the roughness estimation based on skin deformation is comparable to that based on groove width. Macroscopic surface features characterized by groove width can typically predict subjective roughness with correlation coefficients of almost 1 ($r = .96$–$.99$) [3], [5], [7], [26]. Estimates based on skin deformation are not expected to exhibit correlation coefficients higher than these values. Earlier studies successfully estimated roughness intensities using the spatial variation in the activity of SAI units or their spatial spectral components [3], [19]–[21]. This study computed the spatial spectra of skin deformation and revealed that skin spectral components are closely correlated to subjective roughness. This result is intuitive considering that Merkel discs exist immediately beneath the superficial layer of the skin; however, this relationship has not been demonstrated previously. Therefore, assuming that the observed skin deformation is applicable to a variety of surface textures, which requires further experimental verification, this relationship has important industrial applications for material and surface design.

In this study, we used the optimal value of λ for each individual participant. It is natural that λ depends on individuals owing to differences in the biomechanical properties of fingers. Any difference in the mechanical properties of skin will lead to a difference in its

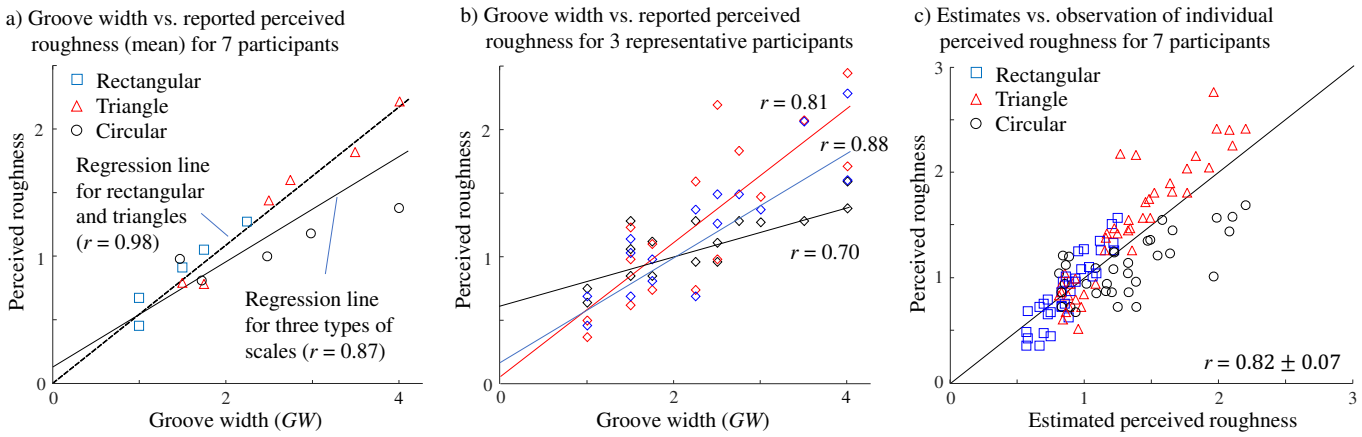

Fig. 5. Subjective roughness vs. grating width. a) Mean subjective roughness from 7 participants vs. groove width. The dotted line is a regression line for the rectangular and triangular gratings, for which 77 samples were used. The solid line is a regression line for the three types of grating scales, for which 112 samples were used. b) Subjective roughness vs. groove width for three individuals and their regression lines. Each regression is based on 16 samples. They include the lines of highest and lowest gradients. Different colors correspond to different participants. The same participants appear in Fig. 6a. c) Reported and estimated roughness values for 112 samples. The solid line indicates the match between the estimated and reported perceived roughness.

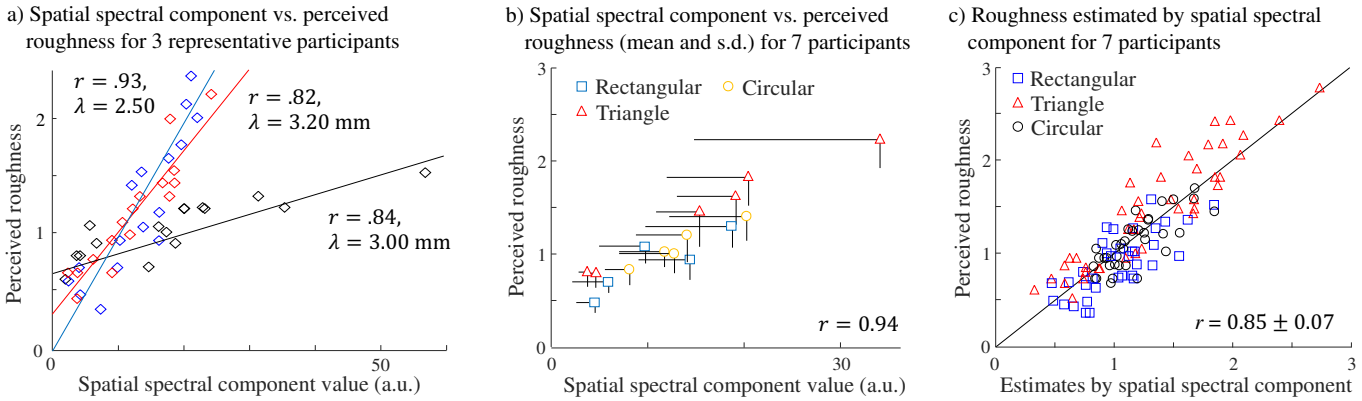

Fig. 6. Subjective roughness estimated by the spatial spectral component of skin. a) Reported subjective roughness vs. spectral component for three participants including those with the highest and lowest gradients defined by linear regression. Only three participants are shown for visual clarity and 16 samples were used for each regression. The same participants appear in Fig. 5b. b) Means and standard errors of subjective roughness and spectral components computed from 112 samples of 7 participants. c) Estimated and reported roughness values for 112 samples of 7 participants. The line represents an exact correlation between reported and estimated roughness intensities.

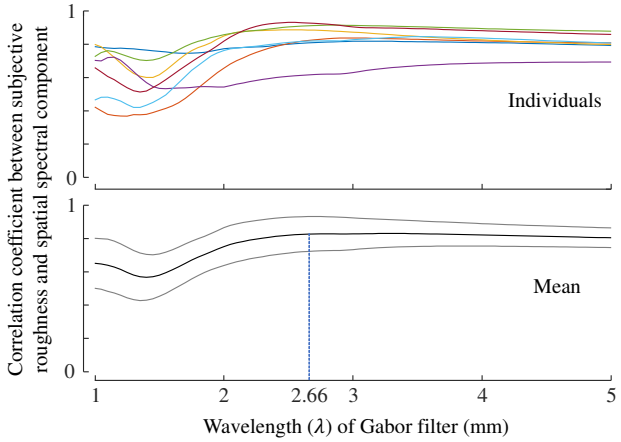

Fig. 7. Top) Correlation coefficients between subjective roughness and spatial spectral components computed using the Gabor filter of λ. Each color corresponds to a different participant. Bottom) Mean and standard deviations of the correlation coefficients of all study participants. The mean correlation is maximum at $\lambda = 2.66$ mm.

spatial filter effect [27]. Finger size particularly affects the sensitivity of spatial pattern recognition [28]. It will be interesting to investigate the determinants of λ in future. Finger size and softness may potentially influence λ.

In our experiments, spatial components and subjective roughness exhibited a close correlation ($r \geq 0.82$, lower panel of Fig. 7) in the range of $\lambda = 2.45$–4.00 mm,. If a specific value of λ is strongly preferred over other values, subjective roughness should exhibit a clear peak intensity for gratings with the spatial period of that value of λ. However, previous studies do not exhibit such phenomena. A few studies have reported roughness intensity as an inverted U-shaped function of groove width with a peak value [3], [5], [10]; however, these peaks were only moderate plateaus. In contrast, Gescheider et al. [29] reported a clear peak of subjective roughness intensity for a dot spacing value of 2.42 mm. In the work of Connor et al. [19], where Gabor filters were applied to the spatial distributions of SAI activities, the correlation coefficient between gross mean subjective roughness and spatial components was larger than 0.90 for $\lambda = 2.0$–4.0 mm. In the study of Blake et al. [20], the optimal λ was within the range of 2.0–3.0 mm (2.6 mm), with which spatial components

accurately estimated subjective roughness. These findings are not inconsistent with other studies where the mean activities of SAI units were used to accurately predict subjective roughness [2], [3], [11], [30]. In brief, the majority of previous research agrees with the findings of this study, i.e., the preferred spatial period ranges from $\lambda = 2.0$–3.0 mm or 2.0–4.0 mm and that this spatial preference is not particularly selective in this wide range.

This study did not include the results for gratings with a groove width of less than 1.0 mm. For these gratings, the peak-to-peak displacement of the pictured skin deformation was limited to several times the spatial resolution (0.014 mm/pixel) of our imaging method. Therefore, future research should improve imaging conditions. Another challenge is the use of nonperiodic roughness scales; the present study employed periodic grating scales. One evident problem of nonperiodic scales is that surface roughness is not homogeneous in a finger–scale contact area, and it is not clear how subjects capture the surface features of such scales. Further, for the extension of the present approach to dynamic touch, we need a totally new approach.

V. Conclusions

Previous studies have highlighted the relationship between perceived macroscopic surface roughness and the spatial variations in the activities of SAI units and the relationship between perceived roughness and macroscopic surface features such as groove width. However, this study is the first to report the relationship between the spatial variations in skin deformation and roughness perception for macroscopic surfaces. This was achieved by computing the spatial spectra of skin deformation using the cross-sectional images of finger pads on different shaped gratings. The spatial spectral components of specific spatial periods were closely correlated with subjective roughness intensities, with a mean correlation coefficient of 0.94. Furthermore, the optimal spatial periods differed among the participants, with a mean of 2.66 mm and a range of 2.45–4.00 mm. Therefore, the strong correlation between roughness perception and spectral components suggests that the peak spatial frequency preferably lies around this point but with a broad range.

References

[1] S. J. Lederman and M. M. Taylor, "Fingertip force, surface geometry, and the perception of roughness by active touch," *Perception & Psychophysics*, vol. 12, no. 5, pp. 401–408, 1972.

[2] K. Sathian, A. W.Goodwin, K. T. John, and I. Darian-Smith, "Perceived roughness of a grating: Correlationn with responses of mechanoreceptive afferents innervating the monkey's fingerpad," *Journal of Neuroscience*, vol. 9, no. 4, pp. 1273–1279, 1989.

[3] T. Yoshioka, B. Gibb, A. Dorsch, S. S. Hsiao, and K. O. Johnson, "Neural coding mechanisms underlying perceived roughness of finely textured surfaces," *Journal of Neuroscience*, vol. 21, no. 17, pp. 6905–6916, 2001.

[4] C. J. Cascio and K. Sathian, "Temporal cues contribute to tactile perception of roughness," *Journal of Neuroscience*, vol. 21, no. 14, pp. 5289–5296, 2001.

[5] M. A. Lawrence, R. Kitada, R. L. Klatzky, and S. J. Lederman, "Haptic roughness perception of linear gratings via bare finger or rigid probe," *Perception*, vol. 36, pp. 547–557, 2007.

[6] A. Dépeault, E.-M. Meftah, and C. E. Chapman, "Tactile perception of roughness: Raised-dot spacing, density and disposition," *Experimental Brain Research*, vol. 197, no. 3, pp. 235–244, Aug 2009.

[7] K. Drewing, "Judged roughness as a function of groove frequency and groove width in 3d-printed gratings," in *Haptics: Science, Technology, and Applications*, D. Prattichizzo, H. Shinoda, H. Z. Tan, E. Ruffaldi, and A. Frisoli, Eds. Springer International Publishing, 2018, pp. 258–269.

[8] M. M. Taylor and S. J. Lederman, "Tactile roughness of grooved surfaces: A model and the effect of friction," *Perception & Psychophysics*, vol. 17, no. 1, pp. 23–36, 1975.

[9] C. E. Connor, S. S. Hsiao, J. R. Phillips, and K. O. Johnson, "Tactile roughness: Neural codes that account for psychophysical magnitude estimates," *Journal of Neuroscience*, vol. 10, no. 12, pp. 3823–3836, 1990.

[10] C. E. Chapman, F. Tremblay, W. Jiang, and Lo "Central neural mechanisms contributing to the perception of tactile roughness," *Behavioural Brain Research*, vol. 135, no. 1, pp. 225 – 233, 2002.

[11] A. Sutu, E. Meftah, and E. Chapman, "Physical determinants of the shape of the psychophysical curve relating tactile roughness to raised-dot spacing: Implications for neural coding of roughness," *Journal of Neurophysiology*, vol. 109, no. 5, pp. 1403–1415, 2013.

[12] J. R. Phillips and K. O. Johnson, "Tactile spatial resolution. II. Neural representation of bars, edges, and gratings in monkey primary afferents," *Journal of Neurophysiology*, vol. 46, no. 6, pp. 1192–1203, 1981.

[13] J. R. Phillips, R. S. Johansson, and K. O. Johnson, "Representation of braille characters in human nerve fibres," *Experimental Brain Research*, vol. 81, no. 3, pp. 589–592, Aug 1990.

[14] R. H. LaMotte and M. A. Srinivasan, "Tactile discrimination of shape: responses of slowly adapting mechanoreceptive afferents to a step stroked across the monkey fingerpad," *Journal of Neuroscience*, vol. 7, pp. 1655–1671, 1987.

[15] K. O. Johnson and S. S. Hsiao, "Evaluation of the relative roles of slowly and rapidly adapting afferent fibers in roughness perception," *Canadian Journal of Physiology and Pharmacology*, vol. 72, no. 5, pp. 488–497, 1994.

[16] J. R. Phillips and K. O. Johnson, "Tactile spatial resolution. III. A continuum mechanics model of skin predicting mechanoreceptor responses to bars, edges, and gratings," *Journal of Neurophysiology*, vol. 46, no. 6, pp. 1204–1225, 1981.

[17] M. A. Srinivasan and K. Dandekar, "An investigation of the mechanics of tactile sense using two-dimensional models of the primate fingertip," *Journal Biomechanical Engineering*, vol. 118, no. 1, pp. 48–55, 1996.

[18] D. R. Lesniak and G. J. Gerling, "Predicting SA-I mechanoreceptor spike times with a skin-neuron model," *Mathematical Biosciences*, vol. 220, no. 1, pp. 15–23, 2009.

[19] C. E. Connor and K. O. Johnson, "Neural coding of tactile texture: Comparison of spatial and temporal mechanisms for roughness perception," *The Journal of Neuroscience*, vol. 12, no. 9, pp. 3414–3426, 1992.

[20] D. T. Blake, S. S. Hsiao, and K. O. Johnson, "Neural coding mechanisms in tactile pattern recognition: the relative contributions of slowly and rapidly adapting mechanoreceptors to perceived roughness," *Journal of Neuroscience*, vol. 17, no. 19, pp. 7480–7489, 1997.

[21] A. I. Weber, H. P. Saal, J. D. Lieber, J.-W. Cheng, L. R. Manfredi, J. F. I. Dammann, and S. J. Bensmaïa, "Spatial and temporal codes mediate the tactile perception of natural textures," *Proceedings of the National Academy of Sciences*, vol. 110, no. 42, pp. 17 107–17 112, 2013.

[22] M. Hollins and S. J. Bensmaïa, "The coding of roughness," *Canadian Journal of Experimental Psychology*, vol. 61, no. 3, pp. 184–195, 2007.

[23] M. Hollins and S. R. Rinser, "Evidence for the duplex theory of tactile texture perception," *Attention, Perception & Psychophysics*, vol. 62, no. 4, pp. 695–705, 2000.

[24] E. K. Kim, S. A. Wellnitz, S. M. Bourdon, E. A. Lumpkin, and G. J. Gerling, "Force sensor in simulated skin and neural model mimic tactile SAI afferent spiking response to ramp and hold stimuli," *Journal of Neuroengineering and Rehabilitation*, vol. 9, no. 1, p. 45, 2012.

[25] H. P. Saal, B. P. Delhaye, B. C. Rayhaun, and S. J. Bensmaïa, "Simulating tactile signals from the whole hand with millisecond precision," *Journal of Neurophysiology*, vol. 114, no. 28, pp. E5693–E5702, 2017.

[26] N. Kudoh, "Tactile perception of textured surfaces: Eeffects of temporal frequency on perceived roughness by passive touch," *Tohoku Psychologica Folia*, vol. 47, pp. 21–28, 1988.

[27] M. Shimojo, "Mechanical filtering effect of elastic cover for tactile sensor," *IEEE Transactions on Robotics and Automation*, vol. 13, no. 1, pp. 128–132, 1997.

[28] R. M. Peters, E. Hackeman, and D. Goldreich, "Diminutive digits discern delicate details: Fingertip size and the sex difference in tactile spatial acuity," *Journal of Neuroscience*, vol. 29, no. 50, pp. 15 756–15 761, 2009.

[29] G. A. Gescheider, S. J. Bolanowski, T. G. Greenfield, and K. E. Brunette, "Perception of the tactile texture of raised-dot patterns: A multidimensional analysis," *Somatosensory and Motor Research*, vol. 22, no. 3, pp. 127–140, 2005.

[30] M. A. Muniak, S. Ray, S. S. Hsiao, J. F. Dammann, and S. J. Bensmaïa, "The neural coding of stimulus intensity: Linking the population response of mechanoreceptive afferents with psychophysical behavior," *Journal of Neuroscience*, vol. 27, no. 43, pp. 11 687–11 699, 2007.